Electrochemically Controlled Conductance Switching in a Single Molecule: Quinone-Modified Oligo(phenylene vinylene)

Stanislav Tsoi,[†] Igor Griva,[‡] Scott A. Trammell,[†] Amy S. Blum,[†] Joel M. Schnur,[§] and Nikolai Lebedev[†,*]

[†]Center for Bio-Molecular Science and Engineering, Naval Research Laboratory, Washington, D.C. 20375, [‡]Departments of Mathematical and Computational & Data Sciences, George Mason University, Fairfax, Virginia 22030, and [§]College of Science, George Mason University, Fairfax, Virginia 22030

ABSTRACT Reversible conductance switching in single quinone-oligo(phenylene vinylene) (Q-OPV) molecules was demonstrated using electrochemical STM. The switching was achieved by application of electrochemical potential to the substrate supporting the molecule. The ratio of conductances between the high- and low-conductivity states is over 40. The high-conductivity state is ascribed to strong electron delocalization of the fully conjugated hydroquinone-OPV structure, whereas the low-conductivity state is characterized by disruption of electron delocalization in the quinone-OPV structure.

KEYWORDS: quinone · oligo(phenylene vinylene) · self-assembly · electron delocalization · oxidation/reduction · conductance switching · electrochemical STM

The prospect of using molecules as building blocks in novel electronic devices has encouraged an extensive theoretical and experimental search for molecules with specific electron transport properties.[1,2] Among these, the important class of molecular switches describes molecules with two or more stable states of differing electrical conductivity and the ability to toggle the molecule among these states by an external perturbation.[1,2] To date, experimental evidence for voltage-driven[3–9] and optically controlled[10,11] molecular conductance switching has been obtained using a two-terminal configuration. A special case of switching, that is, Coulomb blockade, has been demonstrated for single molecules in a three-electrode configuration, with a gate-controlled molecular conductivity.[12–15] In addition, dramatic examples of electrochemical control of molecular conductivity have been provided by a number of groups.[16–21] In some of the latter studies,[17,18] the change in the molecular conductivity has been attributed to the change of the oxidation state. In this context, recent proposals of a redox-controlled switch based on the quinone motif seem natural.[22,23] The present work reports experimental evidence of the redox-controlled, quinone-based molecular switch.

RESULTS AND DISCUSSION

The molecule investigated, quinone-modified OPV (Q-OPV), consists of a quinone headgroup connected to one end of a phenylene vinylene oligomer, while the other end of the oligomer is functionalized with acetyl-protected thiol for covalent attachment to gold substrates (see Figure 1A). Recent electrochemical investigations in our group revealed that Q-OPV attached to a gold electrode can be reversibly switched between the reduced hydroquinone (HQ-OPV, Figure 1B) and oxidized quinone (Q-OPV, Figure 1C) states by application of an electrochemical potential to the electrode.[24] Thus, in the present study, electrochemical scanning tunneling microscopy (ESTM) was employed to (1) control the oxidation state of Q-OPV and (2) measure electrical conductivity of the molecule on a single-molecule level.

In electrochemical STM, both the tip and sample are immersed in an electrolyte. Application of potential to the sample with respect to a reference electrode allows control of chemical reactions on its surface, while an independent potential applied to the tip results in the tip-sample bias necessary for STM imaging. Consequently, images of the surface are recorded as a function of the sample and tip potentials. In this manner, electrochemical STM combines the ability to control surface chemical reactions with the single-molecule resolution of STM.

Samples for the present study were prepared by the "insertion method" (ref 25 and

*Address correspondence to nlebedev@cbmse.nrl.navy.mil.

Received for review April 15, 2008 and accepted May 12, 2008.

Published online May 28, 2008.
10.1021/nn8002218 CCC: $40.75

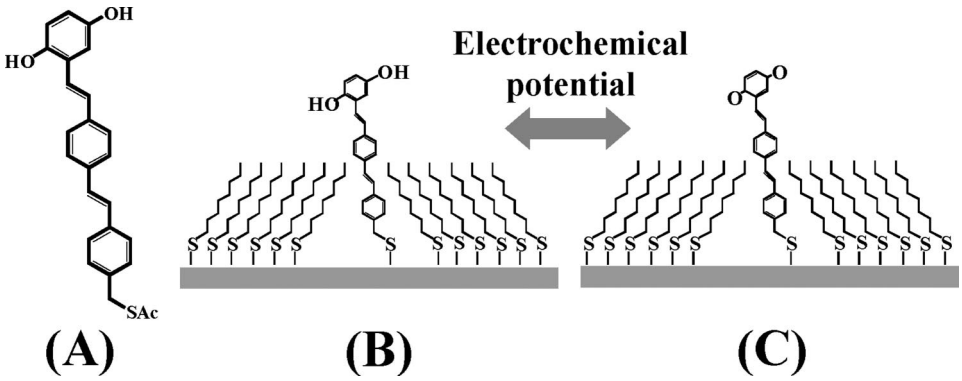

Figure 1. Quinone-OPV with acetyl-protected thiol (A). Q-OPV molecule inserted in octanethiolate SAM at a defect site can be reversibly switched between reduced HQ-OPV (B) and oxidized Q-OPV (C) states by application of electrochemical potential to the substrate.

Figure 1B,C). Figure 2A shows a cyclic voltammogram of a Q-OPV sample. Oxidation and reduction peaks (a redox couple) were observed at around +0.23 V *vs* normal hydrogen electrode (NHE), in agreement with earlier measurements.[24] They were attributed to a proton-coupled, two-electron transfer between the substrate and the quinone headgroup. Thus, the molecule is expected to be reduced (*i.e.*, in HQ-OPV) at substrate potentials more negative than +0.2 V and oxidized (*i.e.*, in Q-OPV) at potentials more positive than +0.3 V *vs* NHE.

An electrochemical STM image recorded from the same Q-OPV sample is shown in Figure 2B. Its main features are protruding (bright) spots on a flat background, the background representing octanethiolate SAM and the spots single Q-OPV molecules or small bunches of molecules inserted in the SAM at defect sites.[25,26] These protruding spots correspond to retraction of the STM tip away from the sample during imaging, which arises from both differences in the physical length and electronic conductivity between the inserted molecule and surrounding alkanethiolate matrix. The amount of retraction is called the apparent height of the inserted molecule (Figure 2C).[27]

Following Bumm *et al.*,[27] one can determine the tunneling decay constant of the inserted molecule from the measurement of its apparent height,[28,29] that is

$$\beta = \frac{\alpha(\Delta h - \Delta\mathrm{STM}) + \beta_{\mathrm{SAM}} l_{\mathrm{SAM}}}{l} \qquad (1)$$

where α and β_{SAM} are the decay constants of the medium in which STM measurements are conducted and SAM, respectively; l and l_{SAM} are physical lengths of the inserted and SAM molecules, respectively; Δh is the difference in the physical heights of the inserted molecule and SAM; and ΔSTM is the measured apparent height. In the present work, we measure the apparent height of Q-OPV over octanethiolate SAM in its two oxidation states and calculate corresponding tunneling decay constants using eq 1.

Two series of ESTM images recorded from two areas of the Q-OPV sample at different substrate and tip potentials are presented in Figure 3A−F. For images A and D, the substrate potential was set to −0.1 V *vs* NHE, resulting in reduction of Q-OPV to HQ-OPV. Simultaneously, the potential of the tip was set to +0.4 V. In the next images (B and E), P_S = +0.3 V, corresponding to oxidation of the inserted molecule to Q-OPV, and P_T = +0.8 V. Finally, for the images C and F, the substrate and tip potentials were brought back to −0.1 and +0.4 V, respectively. The above choice of potentials resulted in the same magnitude and polarity of bias for all images.

Analysis of the apparent heights in images A−F yields distributions shown in Figure 3G−I. Each distribution can be fitted with two Gaussian peaks, their positions presented in the figure. The positions of the peak at greater apparent heights are almost identical in all three distributions, and there are small differences in the positions of the peak at shorter heights. The distributions obtained at the reducing substrate potential (P_S = −0.1 V) are dominated by the peak of greater apparent height, that is, by a state of greater electrical conductivity according to eq 1. In contrast, the state of lower conductivity (shorter apparent height) becomes dominant at the oxidizing substrate potential (P_S = +0.3 V). Such a trend was observed in four other, similarly prepared Q-OPV samples, imaged by different STM tips.

Averaging apparent heights from Figure 3G−I, we obtain $\Delta\mathrm{STM}_1$(average) = 6.1 ± 1.1 Å and $\Delta\mathrm{STM}_2$(average) = 8.3 ± 1.1 Å. Lengths of the octanethiolate and Q-OPV from the terminal carbon atom to the gold surface estimated using the ChemDraw software package[30] are 12.4 and 20.7 Å, respectively, under the assumption that the sulfur−gold bond is 2.4 Å long.[31] Evaluation of Δh yielded 9.3 Å when octanethiolate SAM is assumed to be tilted at 30° with respect to the substrate normal and Q-OPV normal to the surface.[25] We approximate the tunneling decay constant of the buffer by that of water, that is, α = 1.68 ± 0.07 Å^{-1},[32] and an average value of 0.9 Å^{-1} is taken for β_{SAM}.[33,34] With these values, β_1 = 0.80 ± 0.10 Å^{-1} and β_2 = 0.62 ± 0.09 Å^{-1} were obtained using eq 1.

With the decay tunneling constants obtained, one can estimate the on/off ratio of the Q-OPV switch. Resistance of a molecular junction, composed of the substrate, molecule, and tip, is given by $R = R_0 e^{\beta l}$, where R_0 is the contact resistance. Hence $R_{\mathrm{on}}/R_{\mathrm{off}} = R_2/R_1 = \exp[(\beta_2 - \beta_1)l] = 1/41$, that is, the high-conductivity state is more than 40 times more conducting than the low-conductivity state.

Under the experimental conditions employed in the present study, two different electron transport mechanisms can contribute to the observed conductance switching (Figure 4). For the high-conductivity state obtained under the reducing substrate potential, electron transport between the substrate and tip can occur *via* coherent tunneling[35] through the Q-OPV molecule in the reduced HQ-OPV state (Figure 4A′) and resonant tunneling[16,19] mediated by the redox states of the quinone headgroup (Figure 4A). For the low-conductivity state, only coherent tunneling is possible (Figure 4B), as both substrate and tip Fermi levels are below the redox level, its position being known from the CV measurements (Figure 2A).

The contribution from the resonant tunneling (Figure 4A) in the present case, however, may not be significant because electron transfer between the electrodes and quinone headgroup may be slow. Indeed, recent investigations suggested that electron transfer to/from quinone may occur *via* a presumably slow, concerted proton-coupled mechanism.[36] We also note that the value of β_2 (the decay constant of the high-conductivity state) is in perfect agreement with that of OPV3,[28] a molecule structurally similar to HQ-OPV, but lacking the redox states of the quinone headgroup. Thus, it appears that bare coherent tunneling through the molecule in the HQ-OPV state (Figure 4A′) can explain the observed high-conductivity state.

To further corroborate the last conjecture, we performed electronic structure calculations for an isolated Q-OPV molecule in the reduced HQ-OPV and oxidized Q-OPV states (Figure 5). The full aromaticity of hydroquinone is similar to that of the phenyl ring (Figure 1B), resulting in strong electron delocalization along the whole molecule in the reduced HQ-OPV state (Figure 5A,B). In contrast, the disruption of the bond conjugation in quinone (Figure 1C) is responsible for the decreased level of electron delocalization in the oxidized Q-OPV state (Figure 5C,D). As the highest occupied molecular orbital (HOMO) and/or the lowest unoccupied molecular orbital (LUMO) of the molecule defines an effective barrier for coherent tunneling,[37] the more delocalized orbitals of the reduced state should provide a better conductivity path than those of the oxidized state. Hence, the observed conductance switching is likely to originate from the alteration of electron delocalization upon oxidation/reduction of the Q-OPV molecule.

An experiment testing efficiency of coherent tunneling through HQ-OPV would involve application of both the substrate and tip potentials more negative than the redox potential of Q-OPV (+0.23 V *vs* NHE). However, such an experiment was not possible in the present study since application of potentials more negative than +0.4 V *vs* NHE to the tip resulted in occurrence of unwanted electrochemical reactions.

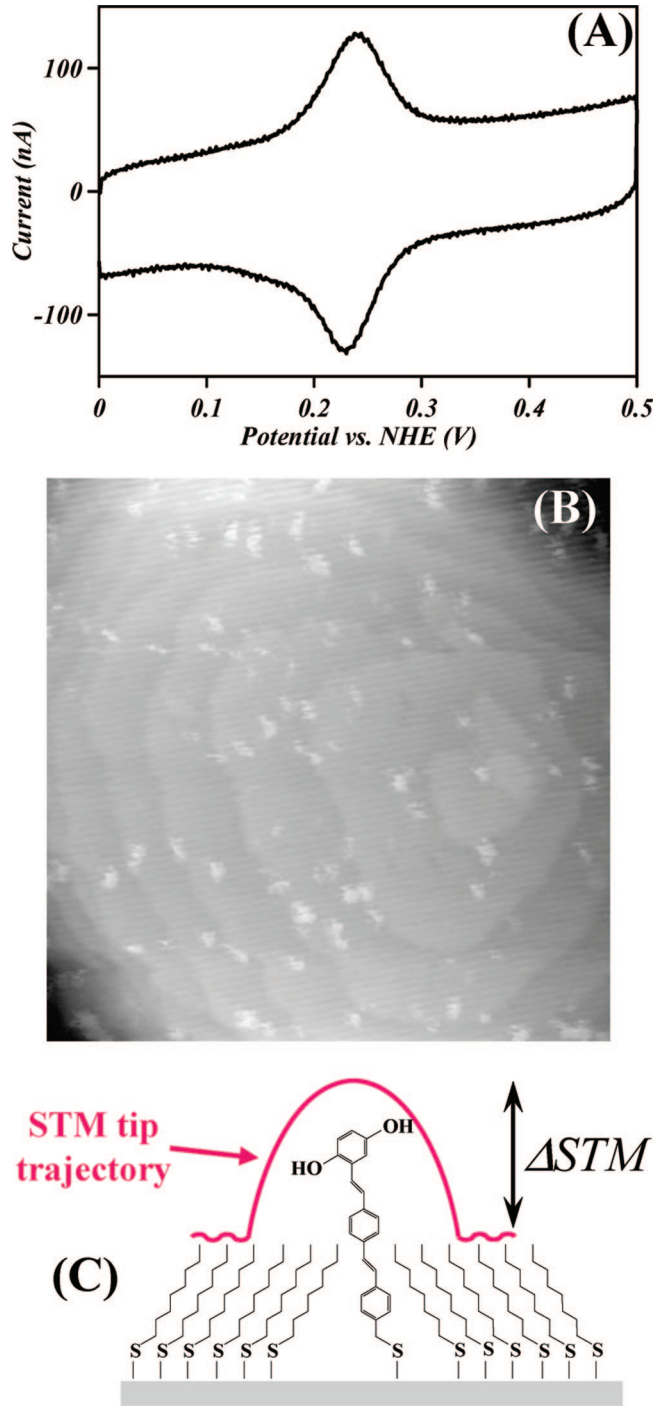

Figure 2. Cyclic voltammogram (A) and ESTM topographic image, 120 × 120 nm^2 (B) of the same Q-OPV sample. The cyclic voltammogram was recorded at 50 mV/s. The ESTM image was obtained with the substrate potential $P_S = -0.1$ V, tip potential $P_T = +0.4$ V (*vs* NHE), and tunneling current $I_t = 13.6$ pA; *z* scale is 5.6 nm (dark to bright). (C) Schematic diagram explaining the origin of protruding spots in the ESTM image. ΔSTM is the apparent height.

Switching of Q-OPV from the high-conductivity state to the low-conductivity state and *vice versa*, observed in the present ESTM images (Figure 3A−F), is not complete, that is, there is a minority of Q-OPV molecules in the low-conductivity state in Figure 3G and I

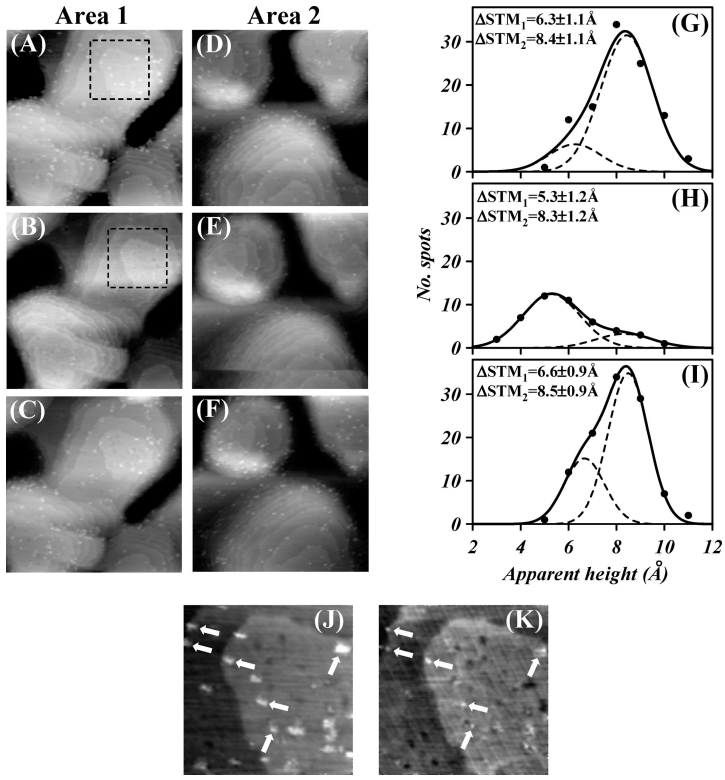

Figure 3. ESTM topographic images (200 × 200 nm^2) recorded from area 1 (A−C) and area 2 (D−F) of the Q-OPV sample. $P_S = -0.1$ V, $P_T = +0.4$ V *vs* NHE (images A, C, D, and F), and $P_S = +0.3$ V, $P_T = +0.8$ V (images B and E). Tunneling current $I_t = 13.6$ pA for all images; *z* scale is 8.8 nm in A−C and 9.5 nm in D−F (dark to bright). (G−I) Distributions of apparent heights measured from images A + D, B + E, and C + F, respectively. Dots are experimental data, lines are Gaussian fits. Images J and K are zoomed in areas designated by squares in images A and B, respectively; arrows indicate the switching molecules.

and a minority in the high-conductivity state in Figure 3H. These unexpected minority fractions are likely to arise from the effect of the tip potential. Indeed, recent ESTM experiments have shown that the potential applied to the tip can shift potential of an investigated molecule,[5] resulting in its unexpected oxidation/reduction. We note, however, that influence of the tip on inserted Q-OPV in the present study is of intermittent nature, as the tip scans over the sample during the experiment. Hence deviations from the expected behavior would be only minor. Another cause of the minority fractions could be trapped local charges, such as defects and impurities, in the vicinity of Q-OPV. A strong local potential of such charges could fix the oxidation state of the molecule, preventing it from switching in response to the substrate potential.

Recent, very careful studies by Moore *et al.* have shown that oligo(phenylene ethynylene) (OPE) molecules inserted in alkane SAM at step edges of gold substrates undergo random movement up and down the step, resulting in measurement of two apparent heights from the same conductivity state, the height difference being equal to 2.4 Å (the height of the atomic step on gold substrates).[38,39] The last value is very close to the apparent height difference reported in the present investigation; however, it is unlikely that the high-conductivity state detected in this study is due to Q-OPV molecules occupying the top of the step edge and the low-conductivity state due to those at the bottom. Indeed, the change of the substrate potential from reducing to oxidizing and *vice versa* changes the apparent height of the most Q-OPVs. In the context of molecular movement up and down the step edge, this would imply that inserted molecules exhibit preference to move up the step at the reducing potential and down at the oxidizing potential. Such a conjecture does not appear reasonable, as the electrostatic potential is constant across the whole substrate. Hence, the high- and low-conductivity states reported here are believed to be due to the two oxidation states of Q-OPV.

In addition to the change in the apparent height of the inserted molecules upon their switching from the high-conductance to low-conductance state and *vice versa*, the number of observed inserted molecules was changing, as well. For instance, the number of total Q-OPV molecules in Figures 3G,H,I was 103, 47, and 107, respectively. Moreover, few molecules detected in Figure 3A are not seen in Figure 3C, even though these images were recorded from the same

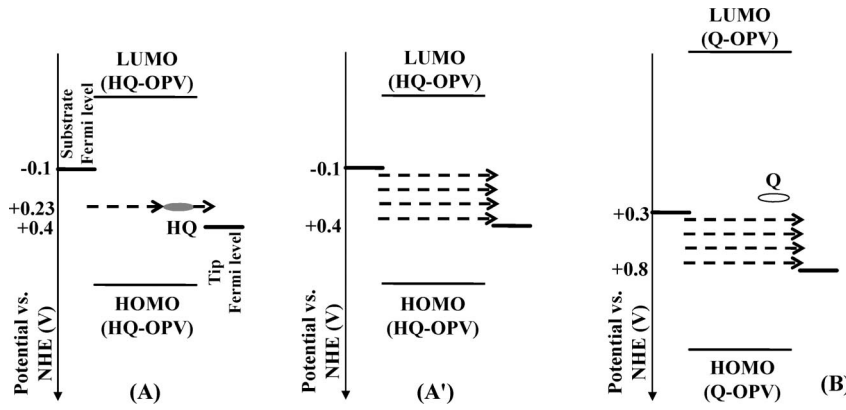

Figure 4. Schematic representation of possible electron transport through Q-OPV molecule for potentials $P_S = -0.1$ V, $P_T = +0.4$ V (A, A′) and $P_S = +0.3$ V, $P_T = +0.8$ V (B) *vs* NHE. HQ =hydroquinone, Q = oxidized quinone. Dashed arrows designate resonant tunneling *via* quinone headgroup (A), coherent tunneling through HQ-OPV (A′), and coherent tunneling through Q-OPV (B). Processes A′ and B differ in the positions of HOMO and LUMO and electron delocalization of the respective structures.

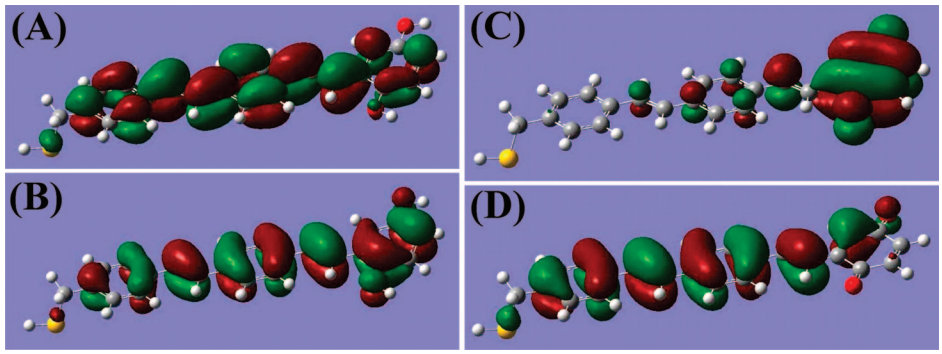

Figure 5. Electron density maps calculated for the lowest unoccupied molecular orbital (LUMO) (A) and the highest occupied molecular orbital (HOMO) (B) of HQ-OPV and LUMO (C) and HOMO (D) of Q-OPV. Energies of the levels *vs* NHE are −2.5 V (A), +0.7 V (B), −0.9 V (C), and +1.1 V (D). Yellow and red balls are sulfur and oxygen atoms, respectively.

area at identical potentials. Such behavior points to stochastic (or spontaneous) switching reported previously for a range of different molecules.[4,9,40,41] An investigation by Ramachandran *et al*. suggested that spontaneous switching was a result of temporary detachment of molecules from the gold substrate.[42] Moore *et al*. have tested several hypothesized mechanisms of stochastic switching and concluded that it was caused by hybridization changes at the molecule−substrate interface.[43] Regardless the real mechanism of stochastic switching, our results suggest that it is affected by application of electrochemical potential to the substrate. We also note that the conductance switching observed in the present work is unlikely to be affected by spontaneous switching because spontaneous switching usually results in the reduction of the conductivity of the inserted molecule to almost that of the surrounding SAM, whereas both the high- and low-conductance states of Q-OPV reported here exhibit significantly better conductivity than SAM.

SUMMARY

The present work experimentally demonstrated operation of the electrochemically controlled, quinone-based molecular switch. Electrochemical oxidation/reduction of its quinone headgroup switches the molecule between the high-conductivity HQ-OPV and low-conductivity Q-OPV states. Our analysis indicates that the switching originates from the alteration of the electronic structure of the switch. The full bond conjugation in HQ-OPV provides an efficient, delocalized tunnel barrier for electron transport. In contrast, the disrupted bond conjugation in Q-OPV is responsible for a weaker electron delocalization with a resultant poorer conductivity. The observed behavior underscores importance of molecular structure on electron transport through molecules and creates foundation for future improved design of molecular switches.

METHODS

Materials. Ethanol (99.5% purity), octanethiol (98.5+ purity), monobasic potassium phosphate (KH_2PO_4), and dibasic potassium phosphate (K_2HPO_4) were purchased from Sigma-Aldrich, and Muscovite mica (grade V-1) was purchased from SPI Supplies. Platinum/iridium wire (0.9Pt/0.1Ir) used to make STM tips was acquired from Nanoscience Instruments, Inc. The synthesis of the Q-OPV molecule is reported elsewhere.[24]

Sample Preparation. Gold substrates were prepared in vacuum (10^{-6} Torr) by electron-beam evaporation of 80 nm of gold on freshly cleaved mica preheated to 250 °C. Atomically flat terraces formed during the deposition were crucial for precise measurement of apparent heights of immobilized molecules. The gold substrate was annealed in hydrogen flame and immersed in 1 mM ethanolic solution of octanethiol for 3 min to form a self-assembled monolayer (SAM). The short incubation time ensured formation of SAM with defect sites available for insertion of Q-OPV. After washing the substrate in ethanol, it was incubated in 0.2 mM solution of Q-OPV in tetrahydrofuran under N_2 atmosphere for 1 h. A small amount of NH_4OH (final concentration ~3 mM) was added to the solution to deprotect the thiol groups. During this step, single Q-OPVs or their small bunches insert in the SAM at defect sites and attach to the substrate *via* gold−thiol bond. Next, the substrate was washed in ethanol, dried in air, and mounted in an open fluid cell for electrochemical STM and cyclic voltammetry measurements.

Measurements. Freshly prepared 10 mM KH_2PO_4/K_2HPO_4 buffer pH 7.0 was used in all experiments. The fluid cell containing the sample was filled with 100 μL of the buffer. Platinum and silver wires mounted inside the cell were employed as the counter and quasi-reference electrodes, respectively, and a bipotentiostat was used for independent control of the substrate and STM tip potentials. First, cyclic voltammetry of the substrate was recorded to determine the position of the quinone redox couple with respect to the quasi-reference. Then, a reducing or oxidizing potential was applied to the substrate, a more positive (by +0.5 V) potential to the tip, and a STM topographic image was recorded. Typically, a series of three images, at reducing, oxidizing, and reducing substrate potentials, was recorded from the same area of the sample to demonstrate reproducibility of the measurements.

STM tips were made by mechanically cutting a Pt/Ir wire. In order to restrict faradaic current flowing through the tips, they were coated with Apiezon wax, leaving a small asperity exposed for the detection of the tunneling current. Typical faradaic current did not exceed 5 pA.

The Ag quasi-reference electrode was calibrated by measuring cyclic voltammetry of a similarly prepared Q-OPV sample in the same buffer in a separate electrochemical cell against an Ag/AgCl reference electrode. The position of the quinone redox couple was *ca*. +0.23 V *vs* NHE. Thus, all cyclic voltammetry

curves recorded inside the STM fluid cell were corrected to obtain the correct position for the quinone redox couple.

Electronic Structure Calculations. Molecular geometry optimization and electronic structure calculations based on density functional theory for reduced HQ-OPV and oxidized Q-OPV were carried out with B3LYP nonlocal exchange-correlation functional comprising Becke's three-parameter exchange functional[44] and the Lee−Yang−Parr correlation functional,[45] using Gaussian software[46] with the B3LYP6-31g(d) basis set.

Acknowledgment. This work was supported in part by NRL NanoScience Institute, Air Force Office of Scientific Research, and the Office of Naval Research *via* the NRL base program. The authors thank K. Kudin for his valuable comments and suggestions that helped improve the accuracy of the electronic structure calculations.

REFERENCES AND NOTES

1. Joachim, C.; Gimzewski, J. K.; Aviram, A. Electronics Using Hybrid-Molecular and Mono-Molecular Devices. *Nature* **2000**, *408*, 541–548.
2. Weibel, N.; Grunder, S.; Mayor, M. Functional Molecules in Electronic Circuits. *Org. Biomol. Chem.* **2007**, *5*, 2343–2353.
3. Li, C.; Zhang, D.; Liu, X.; Han, S.; Tang, T.; Zhou, C.; Fan, W.; Koehne, J.; Han, J.; Meyyappan, M.; Rawlett, A. M.; Price, D. W.; Tour, J. M. Fabrication Approach for Molecular Memory Arrays. *Appl. Phys. Lett.* **2003**, *82*, 645–647.
4. Blum, A. S.; Kushmerick, J. G.; Long, D. P.; Patterson, C. H.; Yang, J. C.; Henderson, J. C.; Yao, Y.; Tour, J. M.; Shashidhar, R.; Ratna, B. R. Molecularly Inherent Voltage-Controlled Conductance Switching. *Nat. Mater.* **2005**, *4*, 167–172.
5. Cai, L.; Cabassi, M. A.; Yoon, H.; Cabarcos, O. M.; McGuiness, C. L.; Flatt, A. K.; Allara, D. L.; Tour, J. M.; Mayer, T. S. Reversible Bistable Switching in Nanoscale Thiol-Substituted Oligoaniline Molecular Junctions. *Nano Lett.* **2005**, *5*, 2365–2372.
6. Lewis, P. A.; Inman, C. E.; Maya, F.; Tour, J. M.; Hutchison, J. E.; Weiss, P. S. Molecular Engineering of The Polarity and Interactions of Molecular Electronic Switches. *J. Am. Chem. Soc.* **2005**, *127*, 17421–17426.
7. He, J.; Fu, Q.; Lindsay, S.; Ciszek, J. W.; Tour, J. M. Electrochemical Origin of Voltage-Controlled Molecular Conductance Switching. *J. Am. Chem. Soc.* **2006**, *128*, 14828–14835.
8. Dichtel, W. R.; Heath, J. R.; Stoddart, J. F. Designing Bistable [2]Rotaxanes for Molecular Electronic Devices. *Philos. Trans. R. Soc. A* **2007**, *365*, 1607–1625.
9. Blum, A. S.; Soto, C. M.; Wilson, C. D.; Amsinck, C.; Franzon, P.; Ratna, B. R. Electronic Properties of Molecular Memory Circuits on a Nanoscale Scaffold. *IEEE Trans. Nanobiosci.* **2007**, *6*, 270–274.
10. He, J.; Chen, F.; Liddell, P. A.; Andreasson, J.; Straight, S. D.; Gust, D.; Moore, T. A.; Moore, A. L.; Li, J.; Sankey, O. F.; Lindsay, S. M. Switching of a Photochromic Molecule on Gold Electrodes: Single-Molecule Measurements. *Nanotechnology* **2005**, *16*, 695–702.
11. Katsonis, N.; Kudernac, T.; Walko, M.; van der Molen, S. J.; van Wees, B. J.; Feringa, B. L. Reversible Conductance Switching of Single Diarylethenes on a Gold Surface. *Adv. Mater.* **2006**, *18*, 1397–1400.
12. Park, J.; Pasupathy, A. N.; Goldsmith, J. I.; Chang, C.; Yaish, Y.; Petta, J. R.; Rinkoski, M.; Sethna, J. P.; Abruna, H. D.; McEuen, P. L.; Ralph, D. C. Coulomb Blockade and the Kondo Effect in Single-Atom Transistors. *Nature* **2002**, *417*, 722–725.
13. Kubatkin, S.; Danilov, A.; Hjort, M.; Cornil, J.; Bredas, J.-L.; Stuhr-Hansen, N.; Hedegard, P.; Bjornholm, T. Single-Electron Transistor of a Single Organic Molecule With Access to Several Redox States. *Nature* **2003**, *425*, 698–701.
14. Natelson, D.; Yu, L. H.; Ciszek, J. W.; Keane, Z. K.; Tour, J. M. Single-Molecule Transistors: Electron Transfer in the Solid State. *Chem. Phys.* **2006**, *324*, 267–275.
15. Ahn, C. H.; Bhattacharya, A.; Di Ventra, M.; Eckstein, J. N.; Frisbie, C. D.; Gershenson, M. E.; Goldman, A. M.; Inoue, I. H.; Mannhart, J.; Millis, A. J.; Morpurgo, A. F.; Natelson, D.; Triscone, J.-M. Electrostatic Modification of Novel Materials. *Rev. Mod. Phys.* **2006**, *78*, 1185–1212.
16. Tao, N. J. Probing Potential-Tuned Resonant Tunneling Through Redox Molecules with Scanning Tunneling Microscopy. *Phys. Rev. Lett.* **1996**, *76*, 4066–4069.
17. Haiss, W.; van Zalinge, H.; Higgins, S. J.; Bethel, D.; Hobenreich, H.; Schiffrin, D. J.; Nichols, R. J. Redox State Dependence of Single Molecule Conductivity. *J. Am. Chem. Soc.* **2003**, *125*, 15294–15295.
18. Chen, F.; He, J.; Nuckolls, C.; Roberts, T.; Klare, J. E.; Lindsay, S. A Molecular Switch Based on Potential-Induced Changes of Oxidation State. *Nano Lett.* **2005**, *5*, 503–506.
19. Albrecht, T.; Guckian, A.; Ulstrup, J.; Vos, J. G. Transistor-Like Behavior of Transition Metal Complexes. *Nano Lett.* **2005**, *5*, 1451–1455.
20. Yokota, Y.; Miyazaki, A.; Fukui, K.; Enoki, T.; Hara, M. In Situ STM Study of Potential-Dependent Height Change of a Tetrathiafulvalene Derivative Embedded in Alkanethiol Self-Assembled Monolayers on Au(111). *J. Phys. Chem. B* **2005**, *109*, 23779–23782.
21. Albrecht, T.; Guckian, A.; Kuznetsov, A. M.; Vos, J. G.; Ulstrup, J. Mechanism of Electrochemical Charge Transport in Individual Transition Metal Complexes. *J. Am. Chem. Soc.* **2006**, *128*, 17132–17138.
22. Sorensen, J. K.; Vestergaard, M.; Kadziola, A.; Kilsa, K.; Nielsen, M. B. Synthesis of Oligo(Phenyleneethynylene)-Tetrathiafulvalene Cruciforms for Molecular Electronics. *Org. Lett.* **2006**, *8*, 1173–1176.
23. van Dijk, E. H.; Myles, D. J. T.; van der Veen, M. H.; Hummelen, J. C. Synthesis and Properties of an Anthraquinone-Based Redox Switch for Molecular Electronics. *Org. Lett.* **2006**, *8*, 2333–2336.
24. Trammell, S. A.; Seferos, D. S.; Moore, M.; Lowy, D. A.; Bazan, G. C.; Kushmerick, J. G.; Lebedev, N. Rapid Proton-Coupled Electron-Transfer of Hydroquinone Through Phenylenevinylene Bridges. *Langmuir* **2007**, *23*, 942–948.
25. Bumm, L. A.; Arnold, J. J.; Cygan, M. T.; Dunbar, T. D.; Burgin, T. P.; Jones, L., II; Allara, D. L.; Tour, J. M.; Weiss, P. S. Are Single Molecular Wires Conducting? *Science* **1996**, *271*, 1705–1707.
26. A rough estimate, made from a comparison of the charge exchanged between the substrate and Q-OPVs in a single oxidation/reduction wave (Figure 2A) and the number of spots seen in ESTM images (Figure 2B), shows that each spot contains fewer than three Q-OPV molecules on average.
27. Bumm, L. A.; Arnold, J. J.; Dunbar, T. D.; Allara, D. L.; Weiss, P. S. Electron Transfer Through Organic Molecules. *J. Phys. Chem. B* **1999**, *103*, 8122–8127.
28. Moth-Poulsen, K.; Patrone, L.; Stuhr-Hansen, N.; Christensen, J. B.; Bourgoin, J.-P.; Bjornholm, T. Probing the Effects of Conjugation Path on the Electronic Transmission Through Single Molecules Using Scanning Tunneling Microscopy. *Nano Lett.* **2005**, *5*, 783–785.
29. Seferos, D. S.; Blum, A. S.; Kushmerick, J. G.; Bazan, G. C. Single-Molecule Charge-Transport Measurements That Reveal Technique-Dependent Perturbations. *J. Am. Chem. Soc.* **2006**, *128*, 11260–11267.
30. *ChemDraw Ultra1*, version 6.0.1; CambridgeSoft: Cambridge, MA, 2000.
31. Esplandiu, M. J.; Carot, M. L.; Cometto, F. P.; Macagno, V. A.; Patrito, E. M. Electrochemical STM Investigation of 1,8-Octanedithiol Monolayers on Au(111). Experimental and Theoretical Study. *Surf. Sci.* **2006**, *600*, 155–172.
32. Ponce, A.; Gray, H. B.; Winkler, J. R. Electron Tunneling Through Water: Oxidative Quenching of Electronically Excited $Ru(tpy)_2^{2+}$ by Ferric Ions in Aqueous Glasses at 77K. *J. Am. Chem. Soc.* **2000**, *122*, 8187–8191.
33. Wold, D. J.; Haag, R.; Rampi, M. A.; Frisbie, C. D. Distance Dependence of Electron Tunneling Through Self-Assembled Monolayers Measured by Conducting Probe Atomic Force Microscopy: Unsaturated *versus* Saturated

Molecular Junctions. *J. Phys. Chem. B* **2002**, *106*, 2813–2816.
34. Li, X.; He, J.; Hihath, J.; Xu, B.; Lindsay, S. M.; Tao, N. J. Conductance of Single Alkanedithiols: Conduction Mechamism and Effect of Molecule-Electrode Contacts. *J. Am. Chem. Soc.* **2006**, *128*, 2135–2141.
35. McCreery, R. L. Molecular Electronic Junctions. *Chem. Mater.* **2004**, *16*, 4477–4496.
36. Costentin, C.; Robert, M.; Saveant, J.-M. Carboxylates as Proton-Accepting Groups in Concerted Proton-Electron Transfers. Electrochemistry of the 2,5-Dicarboxylate 1,4-Hydrobenzoquinone/2,5-Dicarboxy 1,4-Benzoquinone Couple. *J. Am. Chem. Soc.* **2006**, *128*, 8726–8727.
37. Kushmerick, J. G.; Allara, D. L.; Mallouk, T. E.; Mayer, T. S. Electrical and Spectroscopic Characterization of Molecular Junctions. *MRS Bull.* **2004**, 396–402.
38. Moore, A. M.; Mantooth, B. A.; Donhauser, Z. J.; Maya, F.; Price, D. W., Jr.; Yao, Y.; Tour, J. M.; Weiss, P. S. Cross-Step Place-Exchange of Oligo(Phenylene-Ethynylene) Molecules. *Nano Lett.* **2005**, *5*, 2292–2297.
39. Moore, A. M.; Mantooth, B. A.; Donhauser, Z. J.; Yao, Y.; Tour, J. M.; Weiss, P. S. Real-Time Measurements of Conductance Switching and Motion of Single Oligo(Phenylene Ethynylene) Molecules. *J. Am. Chem. Soc.* **2007**, *129*, 10352–10353.
40. Donhauser, Z. J.; Mantooth, B. A.; Kelly, K. F.; Bumm, L. A.; Monnell, J. D.; Stapleton, J. J.; Price, D. W., Jr.; Rawlett, A. M.; Allara, D. L.; Tour, J. M.; Weiss, P. S. Conductance Switching in Single Molecules Through Conformational Changes. *Science* **2001**, *292*, 2303–2307.
41. Wassel, R. A.; Fuierer, R. R.; Kim, N.; Gorman, C. B. Stochastic Variation in Conductance on the Nanometer Scale: A General Phenomenon. *Nano Lett.* **2003**, *3*, 1617–1620.
42. Ramachandran, G. K.; Hopson, T. J.; Rawlett, A. M.; Nagahara, L. A.; Primak, A.; Lindsay, S. M. A Bond-Fluctuation Mechanism for Stochastic Switching in Wired Molecules. *Science* **2003**, *300*, 1413–1416.
43. Moore, A. M.; Dameron, A. D.; Mantooth, B. A.; Smith, R. K.; Fuchs, D. J.; Ciszek, J. W.; Maya, F.; Yao, Y.; Tour, J. M.; Weiss, P. S. Molecular Engineering and Measurements to Test Hypothesized Mechanisms in Single Molecule Conductance Switching. *J. Am. Chem. Soc.* **2006**, *128*, 1959–1967.
44. Becke, A. D. Density-Functional Thermochemistry. III. The Role of Exact Exchange. *J. Chem. Phys.* **1993**, *98*, 5648–5652.
45. Lee, C.; Yang, W.; Parr, R. G. Development of the Colle-Salvetti Correlation-Energy Formula into a Functional of the Electron Density. *Phys. Rev. B* **1988**, *37*, 785–789.
46. Frisch, M. J. *Gaussian 03*, revision C.02; Gaussian, Inc.: Wallingford, CT, 2004.